Optics & Laser Technology 44 (2012) 1026–1030

Contents lists available at SciVerse ScienceDirect

Optics & Laser Technology

journal homepage: www.elsevier.com/locate/optlastec

1.3-μm InGaAsP planar buried heterostructure laser diodes with AlInAs electron stopper layer

Chia-Lung Tsai [a,*], Chih-Ta Yen [a], Cheng-Yi Chou [a], S.J. Chang [b], Meng-Chyi Wu [c]

[a] Department of Electronic Engineering and Green Technology Research Center, Chang Gung University, Taoyuan, Taiwan
[b] Institute of Microelectronics & Department of Electrical Engineering Center for Micro/Nano Science and Technology Advance Optoelectronic Technology Center, National Cheng Kung University, Tainan, Taiwan
[c] Department of Electrical Engineering, National Tsing-Hua University, Hsinchu, Taiwan

ARTICLE INFO

Article history:
Received 20 September 2011
Received in revised form
14 October 2011
Accepted 15 October 2011
Available online 1 November 2011

Keywords:
InGaAsP BH LDs
Electron stopper layer
Optical fiber communications

ABSTRACT

This study reports on the realization of 1.3-μm InGaAsP buried-heterostructure (BH) laser diodes (LDs) via an Fe-doped semi-insulating InP layer and an AlInAs electron stopper layer (ESL). Experimentally, the as-cleaved BH LD with an AlInAs ESL exhibited improved characteristics in terms of threshold current, slope efficiency, and maximum light output power at 90 °C as compared to those of the normal BH LD without an AlInAs ESL. In addition, high internal quantum efficiency or reduced threshold current density was observed, indicating increased modal gain in BH LDs fabricated with an AlInAs epilayer on top of the active region. It was also found that the temperature sensitivity of the BH LDs with an AlInAs ESL is more stable than that of the normal BH LDs. These results could be attributed to the suppression of thermal carrier leakage out of strain-compensated multiple-quantum-well by a large conduction-band offset of the AlInAs/InGaAsP heterojunction. Otherwise, without consideration of damping factor or coupling loss, the 3-dB bandwidth of the proposed BH LDs reaches a high value of 15.3 GHz. Finally, this TO-can packaged BH LD shows an eye-opening feature with the extinction ratio of 7.49 dB while operating at 10 Gbit/s at 50 mA.

1. Introduction

Due to inherent features such as small cavity volume and high mirror reflectivity; nowadays, light sources based upon 850-nm vertical cavity surface emitting lasers (VCSELs) are capable of fiber–optic communication with data transmission rates of up to 10 Gbit/s [1]. Given propagation loss and chromatic dispersion, practical transmission distances are limited to a very short range (~50 m) for these devices operating at 10 Gbit/s and transmitting in a multimode fiber (MMF) [2]. In contrast, InGaAsP/InP-based strained-layer multiple-quantum-well laser diodes (SL-MQW LDs) are favored for long-distance optical communication due to their low transparent current density, high output power, high differential gain, and high modulation bandwidth [3,4]. Additionally, biaxial strain modifies the valence band structure, which helps alleviate Auger nonradiative recombination process and intervalence band absorption (IVBS). However, InGaAsP/InP LDs have a low conduction band offset (ΔE_c) between the well and barrier layers; consequently, device performance become significantly degraded when LDs operate at high current levels since thermal carriers can easily spillover from the InGaAsP MQWs to barriers or a separate confinement heterostructure (SCH) region.

Postigo et al. [5] have reported the use of InGaAsP/InP short-period superlattices to act as the quantum barrier layers in a 1.3-μm InGaAsP LD. Because the short-period superlattice increases the effective barrier height, a 1200-μm-cavity length LD exhibits improved temperature characteristics (T_0=90 K) in a temperature range from 8 to 40 °C, and the variation in the external differential quantum efficiency has been found to be below 5%. Abraham et al. [6] reported that the amount of carrier leakage out of the active region at high temperature (T=80 °C) is lower for the InGaAsP LDs with an $In_{0.81}Ga_{0.19}P$ electron stopper layer (ESL). Although the slight increase of carrier density in the SCL is detrimental to the lowing of threshold current density, the LDs with an $In_{0.81}Ga_{0.19}P$ ESL still exhibit a comparatively improved internal quantum efficiency. The concept of preventing carrier leakage from the MQW region and preserving the crystalline quality could also be implemented using multiquantum barriers (MQBs) as reported in Ref. [7].

An $Al_{0.48}In_{0.52}As$ lattice matched to an InP layer has a higher conduction band-edge discontinuity (ΔE_c~400 meV) with InGaAsP barrier layers, and is therefore preferentially used here as the ESL in strain-compensated MQWs (SC-MQW) [8]. Furthermore, the rugged surface topography of the LDs was planarized by a Fe-doped semi-insulating current-blocking InP layer using metalorganic chemical vapor deposition (MOCVD). This will simultaneously provide better lateral carrier and optical confinements and facilitate the heat dissipation during LD operations [9].

* Corresponding author.
E-mail address: cltsai@mail.cgu.edu.tw (C.-L. Tsai).

0030-3992/$ - see front matter © 2011 Elsevier Ltd. All rights reserved.
doi:10.1016/j.optlastec.2011.10.015

It is anticipated that the planar buried heterostructure (PBH) LDs with an AlInAs ESL will not only exhibit improved characteristics in terms of threshold current, high power, and high-temperature operation, but will also prove suitable as a medium for high-speed optical fiber communications.

2. Experimental

The schematic cross-section of a 1.3-μm PBH LD is shown in Fig. 1(a). All epitaxial layers were grown on S-doped (100)-oriented InP substrates via a vertical-reactor low-pressure MOCVD system. Trimethylgallium (TMGa) and trimethylindium (TMIn) were used as the group-III sources, while silane (SiH_4), diethyl-zinc (DEZn), and CP_2Fe were, respectively, used as the n-, p-type, and Fe-doping sources. The SC-MQW active region is sandwiched between two 50 nm undoped $In_{0.89}Ga_{0.11}As_{0.24}P_{0.76}$ (λ_g=1.05 μm) SCHs following the epitaxial growth of a 0.3-μm-thick n-type InP buffer layer. The SC-MQW active region consists of eight 5.5-nm-thick $In_{0.90}Ga_{0.10}As_{0.52}P_{0.48}$ wells (λ_g=1.43 μm) with 1% compressive strain (CS) separated by nine −0.25% tensile-strained (TS) $In_{0.85}Ga_{0.15}As_{0.33}P_{0.67}$ barriers (λ_g=1.1 μm, and 8.5 nm thick) for 1.3 μm emission. Because the conduction band offset ratio ($\Delta E_c/\Delta E_g$) of the SC-MQW is only about 0.37, thermal leakage could be suppressed by placing an ESL on top of the active region. Finally, a 250 nm p-InP cladding layer terminates the first growth procedure. Further analysis of the crystalline quality of the as-grown sample can be performed via a JEOL JEM-2100F high-resolution transmission electron microscopy (HRTEM) system with an accelerating voltage of 200 keV. Fig. 1(b) shows the corresponding high-angle annular dark field (HAADF) scanning-TEM (STEM) image of the SC-MQW active region. A 10-nm-thick undoped $Al_{0.48}In_{0.52}As$ (λ_g=0.83 μm) ESL was grown on the p-side adjacent to the InGaAsP MQWs. In addition, the formation of the wavy interface between the well and barrier layers, commonly observed in strained MQW, is not obvious [10]. In the flowing step, standard processes including photolithography and dry etching techniques were used to form a 2-μm-width mesa stripe. Next, the wafer was reloaded to the MOCVD reactor to regrow a Fe-doped current-blocking InP layer with a resistivity of $10^6\ \Omega$ cm. It is known that Zn atoms in p-InP tend to interdiffuse with the Fe-doped InP, and thus the highly-resistant semi-insulating blocking layer becomes more conductive [11]. Experimentally, an additional n-InP layer was grown on top of the Fe-doped InP to protect against the interdiffusion process of Zn and Fe atoms. A nearly flat surface can be obtained after the third regrowth of the p-InP cladding layer along with the p^+-InGaAs contact layer. Finally, the wafer was thinned using mechanical lapping and polishing, and then Cr–AuZn–Au and Au–GeNi–Au metals were deposited to form the p- and n-type

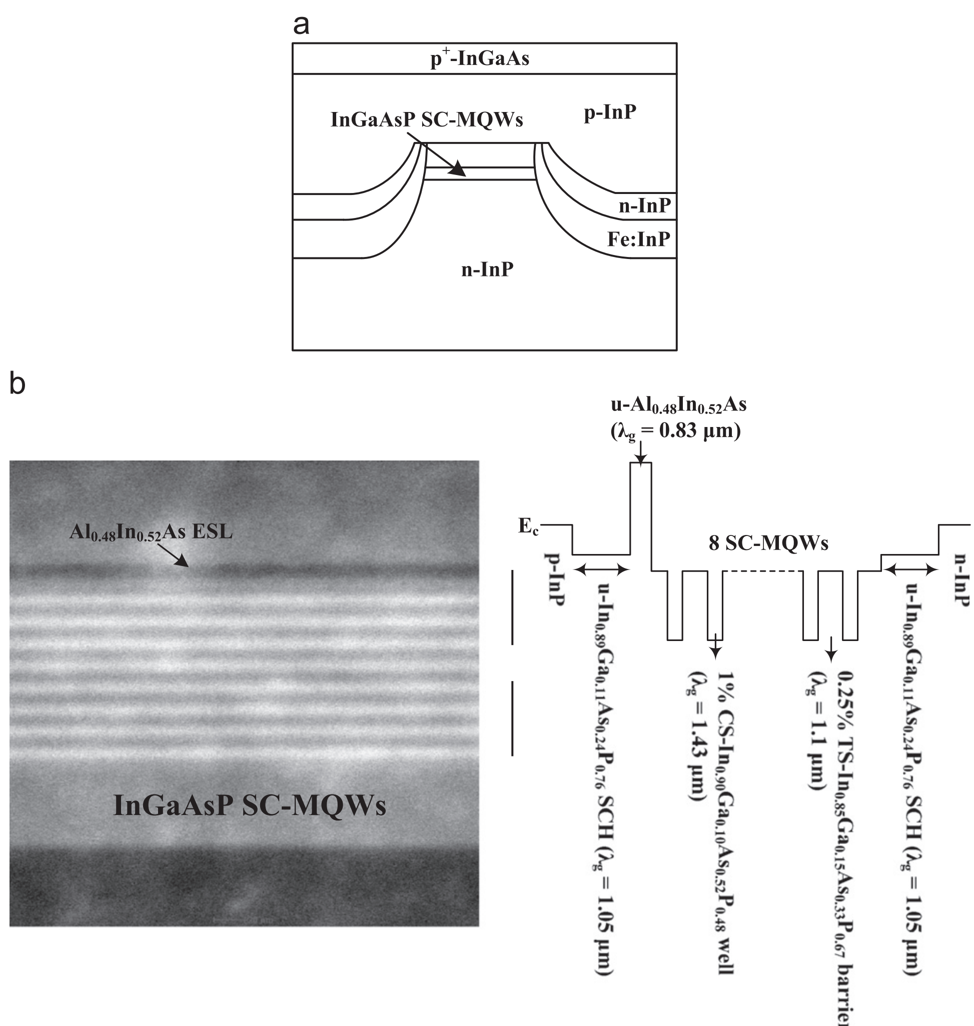

Fig. 1. (a) Schematic cross section of a 1.3-μm planar buried heterostructure (PBH) LD. (b) High-angle annular dark field (HAADF) scanning-TEM (STEM) image of the SC-MQW active region. An additional AlInAs ESL is placed on top of the active region to prevent carrier spillover into the SCH or p-InP cladding layer.